

Supplement of Atmos. Chem. Phys., 21, 1649–1681, 2021
<https://doi.org/10.5194/acp-21-1649-2021-supplement>
© Author(s) 2021. This work is distributed under
the Creative Commons Attribution 4.0 License.



Supplement of

Impacts of multi-layer overlap on contrail radiative forcing

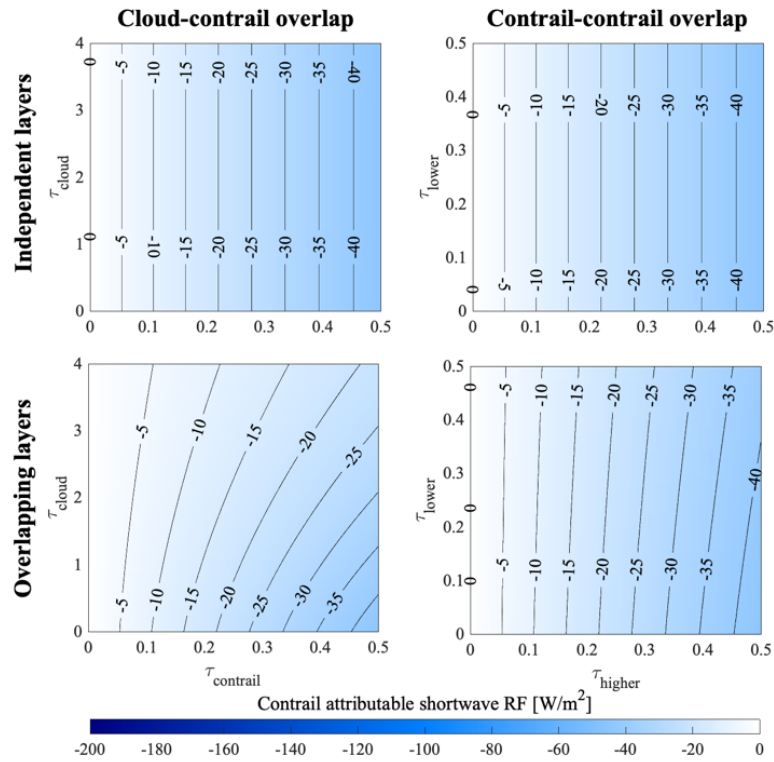
Inés Sanz-Morère et al.

Correspondence to: Sebastian Eastham (seastham@mit.edu)

The copyright of individual parts of the supplement might differ from the CC BY 4.0 License.

Supplementary Information

S1 Additional figures for Section 4.1.1



5

Figure S1. Effect of overlaps on contrail-attributable RF_{SW} as a function of the optical depth τ of each layer. Left: system contrail-contrail; right: system cloud-contrail. Top: contrail RF estimated when treating the layers as independent and summing individual contributions. Bottom: contrail RF estimated in a single calculation which accounts for overlap. Lower and upper contrail properties are the following: asymmetry parameter of 0.77, temperature of 220 K and 215 K respectively. Cloud properties are the following: asymmetry parameter of 0.85, temperature of 260 K. The solar zenith angle (θ) is held at 45° for all cases.

10

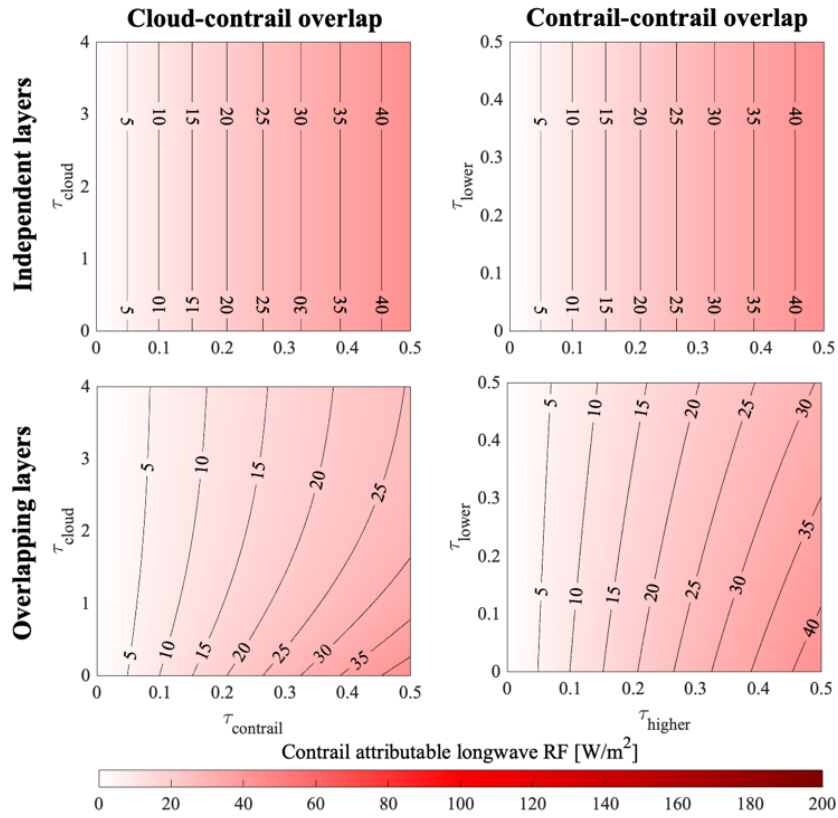
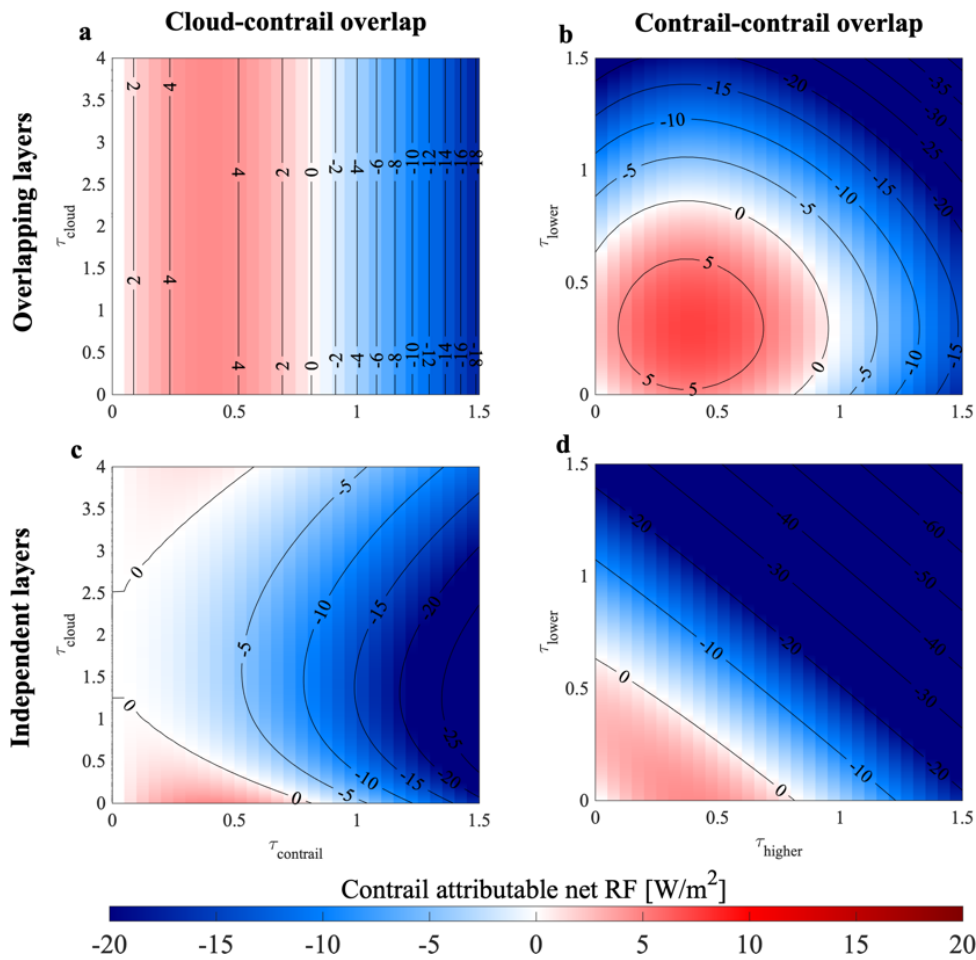


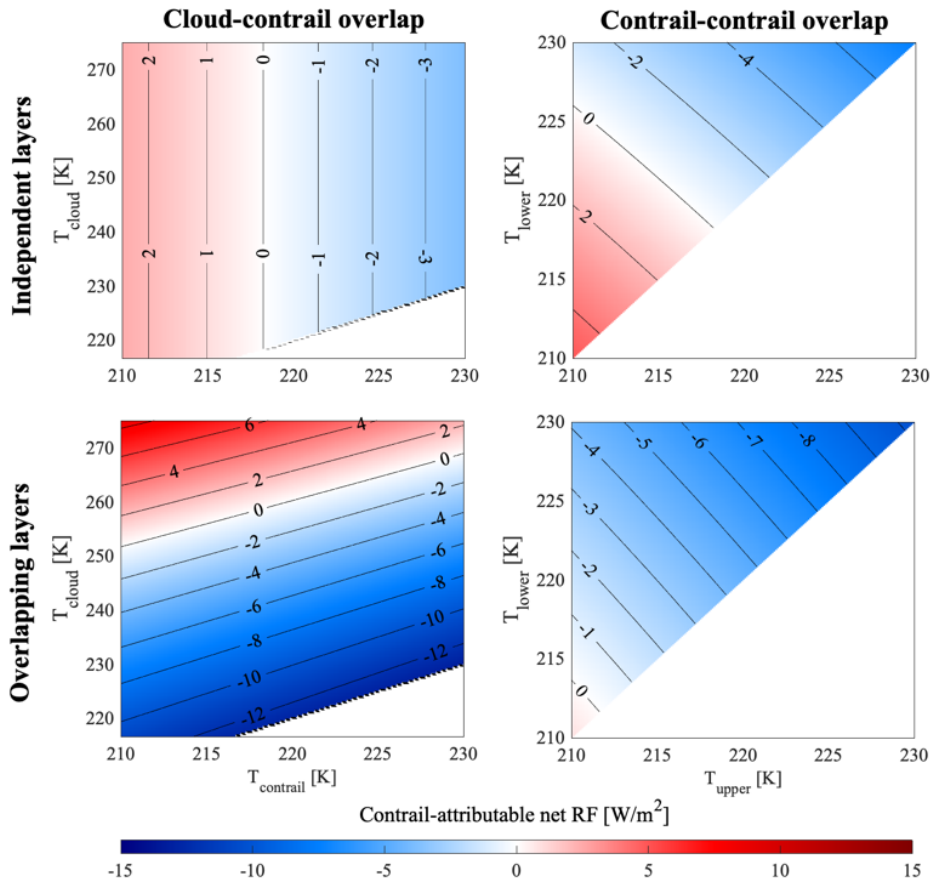
Figure S2. Effect of overlaps on system RFLW varying with optical depth τ . Same properties as Fig. S1.



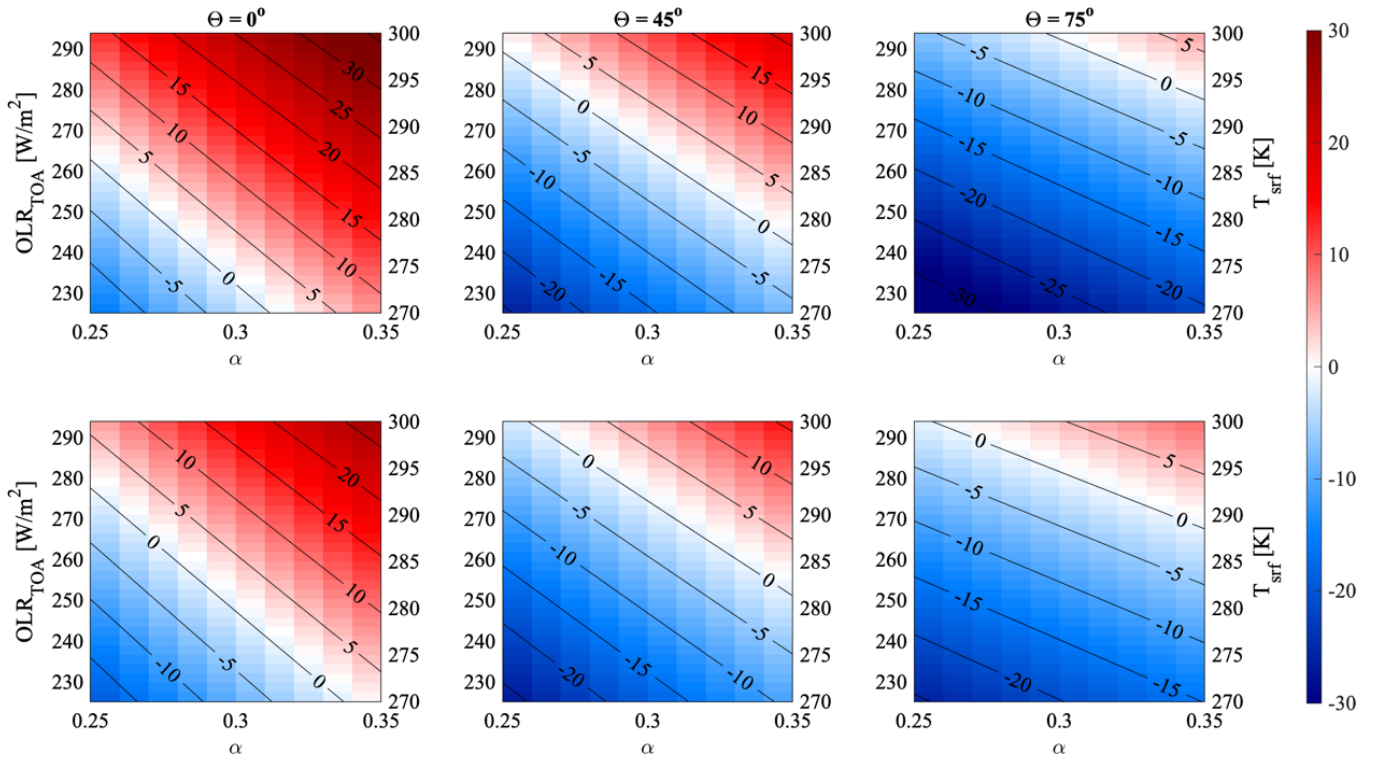
15

Figure S3. Effect of overlap between two layers on the contrail-attributable net RF as a function of optical depth τ . Left: system contrail-contrail; right: system cloud-contrail. Top: contrail RF estimated when treating the layers as independent and summing individual contributions. Bottom: contrail RF estimated in a single calculation which accounts for overlap. Lower and upper contrail properties are the following: asymmetry parameter of 0.77, temperature of 220 K and 215 K respectively. Cloud properties are the following: asymmetry parameter of 0.85, temperature of 260 K. The solar zenith angle $\theta = 30^\circ$ for all calculations.

20



25 **Figure S4.** Effect of overlaps on system net RF varying with layer temperature. Left: system contrail-contrail; right: system cloud-contrail. Top: contrail RF estimated when treating the layers as independent and summing individual contributions. Bottom: contrail RF estimated in a single calculation which accounts for overlap. Lower and upper contrail properties are the following: asymmetry parameter of 0.77, temperature of 220 K and 215 K respectively. Cloud properties are the following: asymmetry parameter of 0.85, temperature of 260 K. The solar zenith angle (θ) is held at 45° for all cases. Cases where the upper layer is warmer than the lower are not shown.



30 **Figure S5.** System contrail-contrail net RF in W/m^2 , varying with local conditions (solar zenith angle θ increasing from left to right, outgoing longwave radiation and Earth surface temperature T_{surf} (based on Corti and Peter, 2009) and albedo α). Upper row: system RF when contrails considered independent. Lower row: system RF when accounting for total overlap. Negative RF is shown in blue and positive RF is shown in red. Lower and upper contrail properties are the following: asymmetry parameter of 0.77, optical depth of 0.3, temperature of 220 K and 215 K respectively.

35

40

45

S2 Additional figure for Section 4.1.2

50

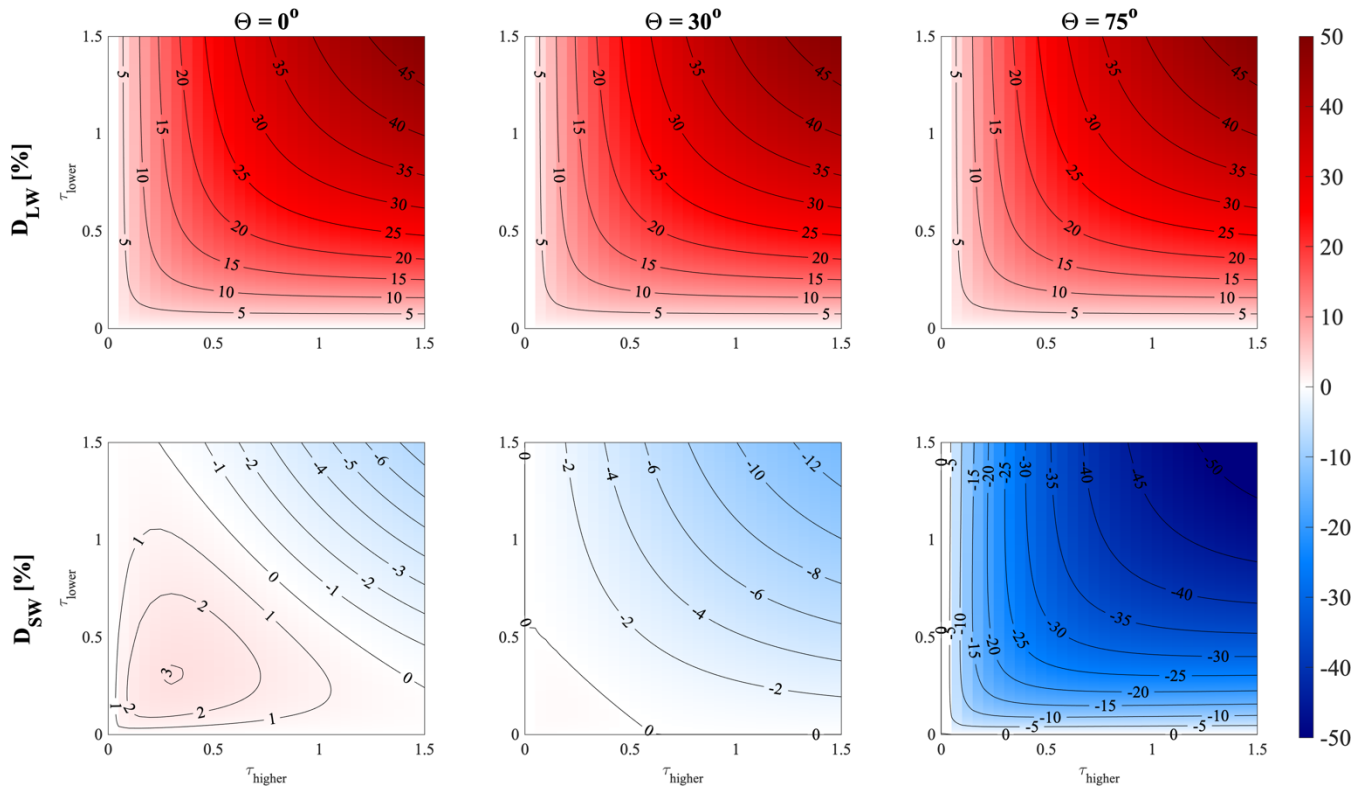


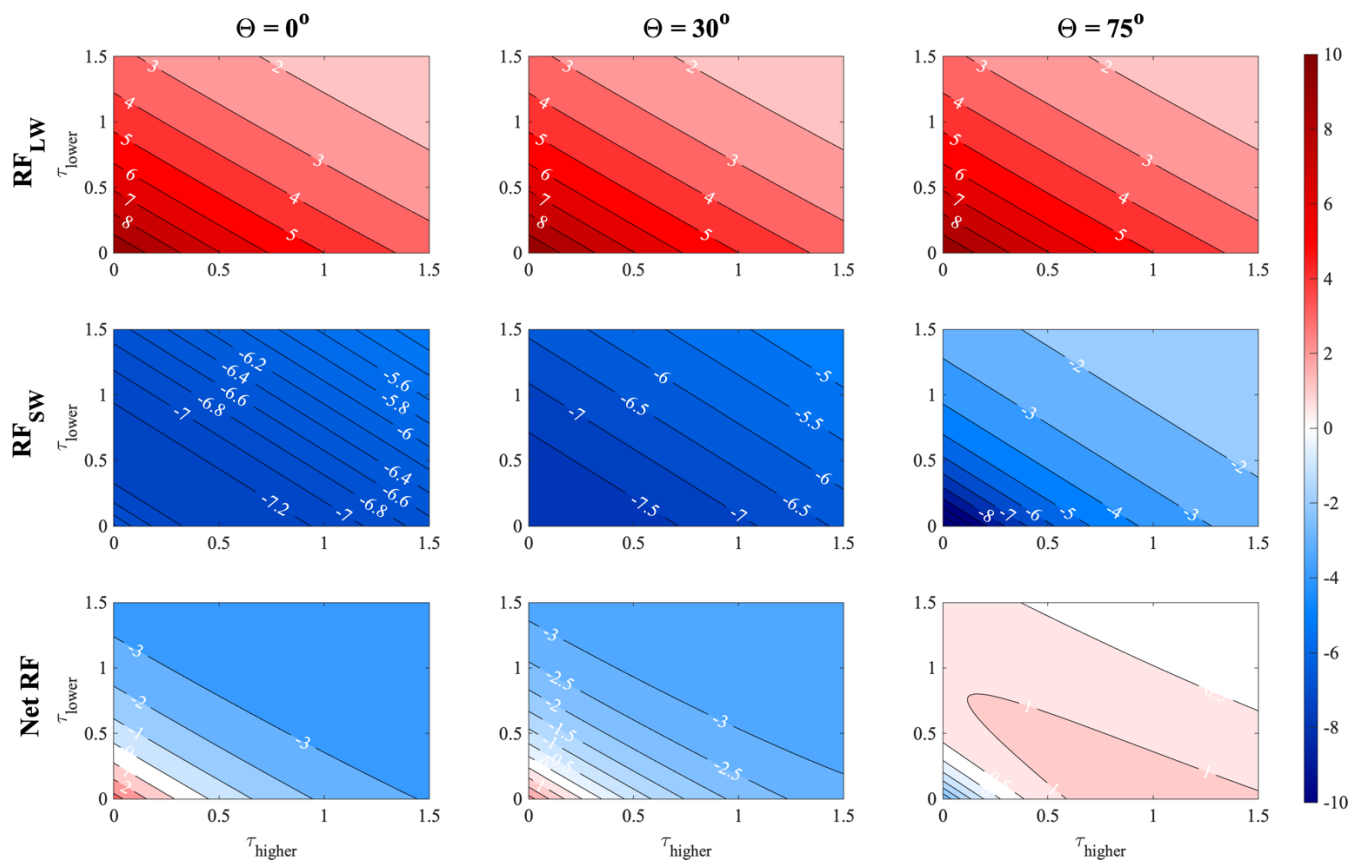
Figure S6. Error in estimated RF for two overlapping contrails when ignoring interaction, as a function of τ and θ . The solar zenith angle increases from the left-most to right-most panels. The upper panels show longwave RF error, while the lower panels show shortwave RF error. Positive (red) values indicate that the independent assumption results in an overestimate of warming effects (or underestimate of cooling effects). Negative (blue) values indicate that the independent assumption results in an overestimate of cooling effects (or underestimate of warming effects).

55

60

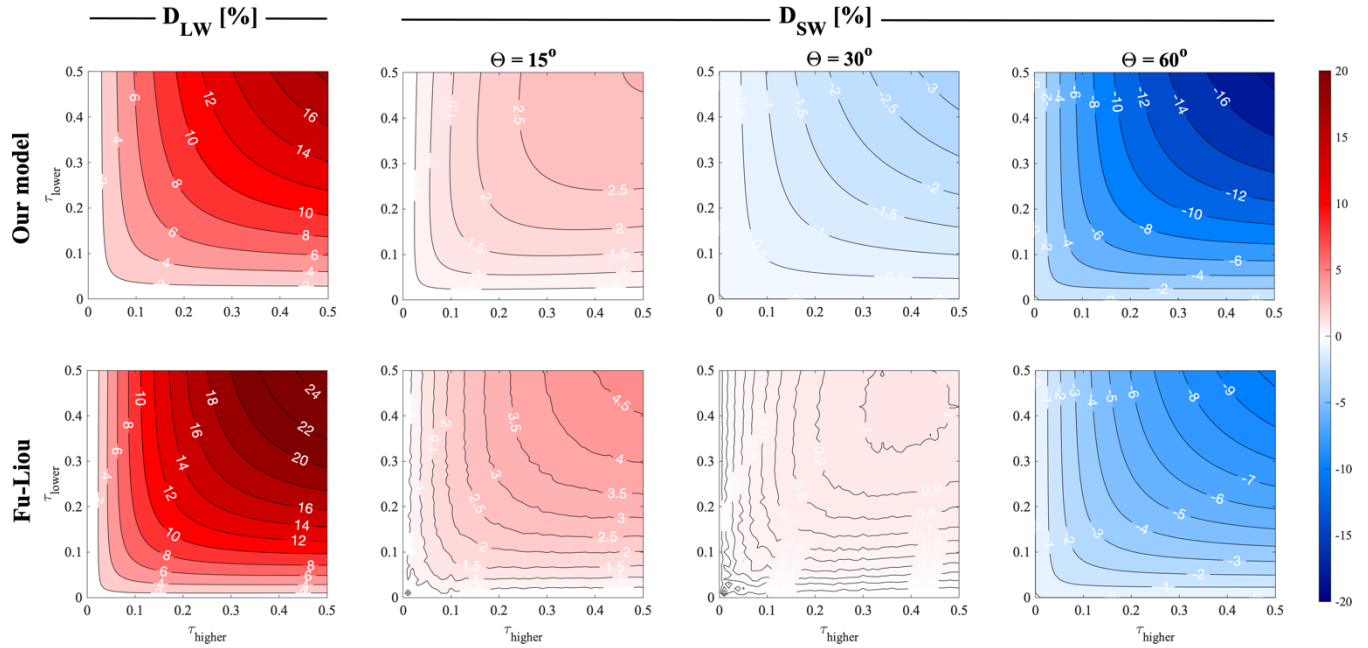
65

S3 Additional figure for Section 4.1.3



75 **Figure S7.** Radiative forcing [W/m²] due to a single contrail between two cirrus cloud layers. Radiative forcing is shown as a function of the solar zenith angle (increasing from left to right) and the optical depth of the lower (Y-axis) and upper (X-axis) natural cloud optical depths. From top to bottom: longwave; shortwave; and net radiative forcing. Contrail optical depth $\tau = 0.1$.

90 S4 Additional figure for Section 4.1.4



95 **Figure S8.** Error in estimated RF for two overlapping contrails when ignoring interaction, as a function of τ and θ , for both our model (upper row of panels) and FL (lower row of panels). The first column shows error in longwave RF, while the remaining columns show error in shortwave RF at different solar zenith angles. Positive (red) values indicate that the independent assumption results in an overestimate of warming effects (or underestimate of cooling effects). Negative (blue) values indicate that the independent assumption results in an overestimate of cooling effects (or underestimate of warming effects).

100

105

110

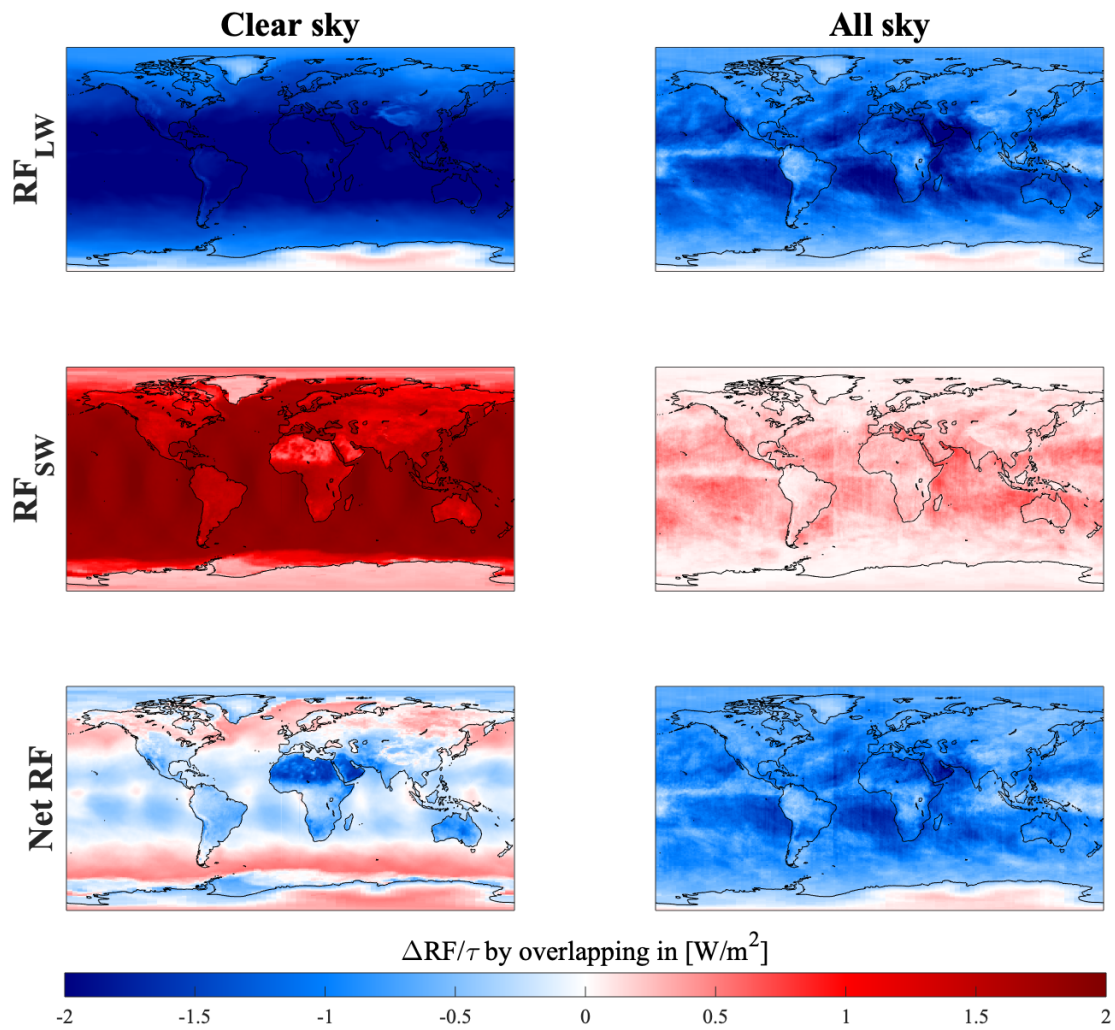
115 **S5 Additional figures for Section 4.2**

120

Table S1. RF from an idealized 1% homogeneous global contrail coverage, as shown in prior literature and in comparison to results from our model. Both clear-sky and all-sky conditions are shown depending on availability. ¹: intercomparison results from Myhre et al. (2009); ²: results are approximated from bar charts given in the original reference; ³: results are provided for three different assumed contrail ice crystal asymmetry parameters, based on observations and as discussed in Sanz-Morère et al. (2020).

Source	RF _{lw}	RF _{sw}	Net RF	RF _{lw}	RF _{sw}	Net RF
	Clear-sky (mW/m ²)			All-sky (mW/m ²)		
Myhre and Stordal (2001)	-	-	-	210	-90	120
Stuber and Forster (2007)	-	-	-	190	-60	130
UiO-BBM ¹	260 ²	-152 ²	108	202	-105	97
UoR-FU ¹	268 ²	-127 ²	131	203	-79	124
UW-FU ¹	275 ²	-127 ²	148	229	-82	147
UoL-E-S ¹	330 ²	-149 ²	181	276	-119	157
CNRM-ARPEGE ¹	370 ²	-150 ²	220	340	-150	190
Frömming et al. (2011)	-	-	-	210	-70	140
Schumann et al. (2012)	-	-	-	213	-117	96
Markowicz and Witek (2013)	-	-	-	200	-70	130
This model ($g \sim 0.7$) ³		-278	-28		-47	97
This model ($g \sim 0.77$) ³	249	-221	28	144	-37	107
This model ($g \sim 0.9$) ³		-105	144		-17	127

Our clear-sky results are consistent with existing values in literature, accounting for the global sensitivity variation due to contrail ice microphysics discussed in Sanz-Morère et al. (2020). All-sky results are consistent in net effect, but the longwave and shortwave terms are smaller in magnitude. This is likely due to the maximum cloud-contrail overlap assumption, which provides an upper bound estimate of the reduction in both shortwave and longwave contrail RF due to the presence of natural clouds.



130 **Figure S9.** Global sensitivity to contrail-contrail overlap ($\Delta RF = RF_O - RF_I$). From top to bottom: longwave, shortwave and net sensitivity to contrail-contrail overlap. Left: clear-sky conditions; right: all-sky conditions (including cloud-contrail overlap effects).

135